

AD-A174 357

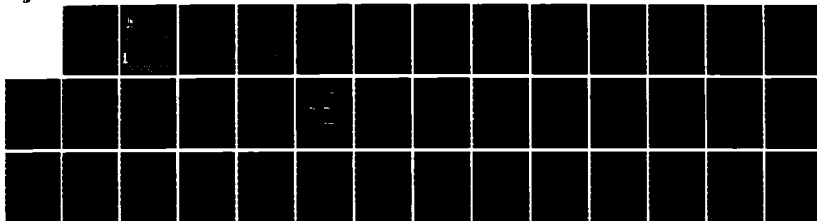
PLASMA THEORY AND SIMULATION(U) CALIFORNIA UNIV  
BERKELEY ELECTRONICS RESEARCH LAB C K BIRDSALL JUN 85  
N00014-77-C-0578

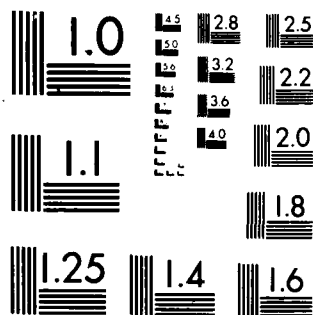
1/1

UNCLASSIFIED

F/G 20/9

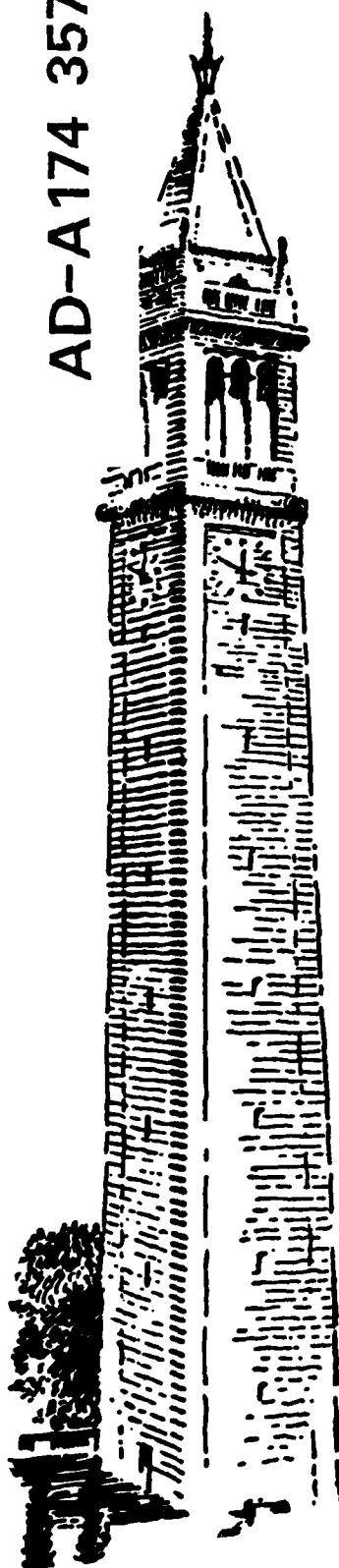
NL





MICROCOPY RESOLUTION TEST CHART  
NATIONAL BUREAU OF STANDARDS-1963-A

AD-A174 357



DTIC FILE COPY

**FIRST & SECOND QUARTER PROGRESS REPORT 1985  
ON PLASMA THEORY AND SIMULATION**

**DTIC  
ELECTE**  
NOV 21 1986

January 1 to June 30, 1985

DOE Contract DE-AS03-76-F00034-DE-AT03-76ET53064  
ONR Contract N00014-77-C-0578  
Varian Gift  
Hughes Aircraft Co. Gift

**DISTRIBUTION STATEMENT A**

Approved for public release;  
Distribution Unlimited

**ELECTRONICS RESEARCH LABORATORY**  
**College of Engineering**  
**University of California, Berkeley, CA 94720**

86 11 21 024

**SECURITY CLASSIFICATION OF THIS PAGE (When Data Entered)**

REPORT DOCUMENTATION PAGE		READ INSTRUCTIONS BEFORE COMPLETING FORM
1. REPORT NUMBER	2. GOVT ACCESSION NO. <b>ADA174357</b>	3. RECIPIENT'S CATALOG NUMBER
4. TITLE (and Subtitle) <b>Quarterly Progress Report 1 of 4 January 1, 1985 - June 30, 1985 USE TITLE ON COVER</b>		5. TYPE OF REPORT & PERIOD COVERED <b>Progress, 1/1 - 6/30, 1985</b>
7. AUTHOR(s) <b>Professor C. K. Birdsall</b>		6. PERFORMING ORG. REPORT NUMBER
9. PERFORMING ORGANIZATION NAME AND ADDRESS <b>Electronics Research Laboratory University of California Berkeley, CA 94720</b>		8. CONTRACT OR GRANT NUMBER(s) <b>ONR N00014-77-C-0578</b>
11. CONTROLLING OFFICE NAME AND ADDRESS <b>ONR Physics Division Department of the Navy, ONR Arlington, VA 22217</b>		10. PROGRAM ELEMENT, PROJECT, TASK AREA & WORK UNIT NUMBERS <b>Element No. 61153N, Project Task Area RR01-09-01, Work Unit No. NR 012-742</b>
14. MONITORING AGENCY NAME & ADDRESS (if different from Controlling Office)		12. REPORT DATE
		13. NUMBER OF PAGES
		15. SECURITY CLASS. (of this report) <b>Unclassified</b>
16. DISTRIBUTION STATEMENT (of this Report)  <b>Approved for public release; distribution unlimited</b>		15a. DECLASSIFICATION/DOWNGRADING SCHEDULE
17. DISTRIBUTION STATEMENT (of the abstract entered in Block 20, if different from Report)		
18. SUPPLEMENTARY NOTES  <b>Our group uses theory and simulation as tools in order to increase the understanding of plasma instabilities, heating, transport, plasma-wall interactions, and large potentials in plasmas. We also work on the improvement of simulation both theoretically and practically.</b>		
19. KEY WORDS (Continue on reverse side if necessary and identify by block number)  <b>Research in plasma theory and simulation, plasma-wall interactions, large potentials in plasmas</b>		
20. ABSTRACT (Continue on reverse side if necessary and identify by block number)		

See reverse side

## 20. ABSTRACT

*General Plasma Theory and Simulation*

- A. *Oblique electron Bernstein wave investigations; linear response limits.* Limits are found for a spatially periodic Vlasov distribution, as a step to understanding the bounded magnetized model.
- B. *Simulation of the effect of large amplitude RF-waves on the interchange instability-supporting theory.* Final report in preparation.
- C. *One-beam Alfvén ion-cyclotron instabilities of multiple ion distribution functions.* Final report in preparation.
- D. *Linear mode coupling in simulations of the Alfvén ion-cyclotron instability.* Final report in preparation.
- E. *Simulations of the weak warm beam-plasma instability: study of the correlation functions.* Final report in preparation.

*Plasma-Wall Physics, Theory and Simulation*

- A. *Transport of particle and energy fluxes through the plasma sheath region, including ion reflection.* The time-independent theory developed is very nearly verified by the average of the time-dependent simulations, with some exceptions.
- B. *Planar magnetron discharges.* The experiment is now running and initial testing is being done, measuring electron density, I-V characteristics at various pressures and B fields. The simulation modelling has added volume creation, electron-neutral collisions (tested to agree with theory) and spatially varying B field.
- C. *Particle simulations of the low-alpha Pierce diode.* The final report is published.
- D. *Thermionic emission I-V paradox.* The problem is described (Longo's 1/J observations) and conjectures are offered on the causes.

*Code Development and Software Distribution*

- A. *POLY: A hybrid scheme for the solution of the Vlasov equation.* One component is modelled by linearized fluid equations and the other component(s) by the full Vlasov equation(s). Application is to E Above.

Accession No.	
DTIC	<input checked="" type="checkbox"/>
DTIC	<input type="checkbox"/>
DTIC	<input type="checkbox"/>
PER CALL JC	
A-1	



DTIC  
ELECTE  
3 NOV 21 1986  
B

## TABLE OF CONTENTS

	Page No.
<b>SECTION I: GENERAL PLASMA THEORY AND SIMULATION</b>	
A. Oblique Electron Bernstein Wave Investigations; Linear Response Limits	1
B. Simulation of the Effect of Large Amplitude RF-Waves on the Interchange Instability-Supporting Theory	1
C. One-Beam Alfvén Ion-Cyclotron Instabilities of Multiple Ion Distribution Functions	1
D. Linear Mode Coupling in Simulations of the Alfvén Ion-Cyclotron Instability	1
E. * Simulations of the Weak Warm Beam-Plasma Instability: Study of the Correlation Functions	1
<b>SECTION II: PLASMA-WALL PHYSICS, THEORY AND SIMULATION</b>	
A. Transport Particle and Energy Fluxes through the Plasma Sheath Region, Including Ion Reflection	3
B. ** Planar Magnetron Discharges	14
C. * Particle Simulations of the Low-Alpha Pierce Diode	15
D. *** Thermionic Emission I-V Paradox	15
<b>SECTION III: CODE DEVELOPMENT AND SOFTWARE DISTRIBUTION</b>	
A. * POLY: A Hybrid Scheme for the Solution of the Vlasov Equation	18
<b>SECTION IV: JOURNAL ARTICLES, REPORTS, VISITORS, TALKS</b>	
<b>DISTRIBUTION LIST</b>	

---

Major support is from DOE.

\* Supported in part by ONR.

\*\* Supported in part by Varian.

\*\*\* Supported in part by Hughes Aircraft Co.

FIRST AND SECOND QUARTER PROGRESS REPORT  
ON  
PLASMA THEORY AND SIMULATION

January 1 to June 30, 1985

*Our research group uses both theory and simulation as tools in order to increase the understanding of instabilities, heating, transport, plasma-wall interactions, and large potentials in plasmas. We also work on the improvement of simulation, both theoretically and practically.*

*Our staff is -*

Professor C. K. Birdsall <i>Principal Investigator</i>	191M	Cory Hall	(643-6631)
Dr. Kim Theilhaber <i>Post-Doctorate; UCB</i>	187M	Cory Hall	(642-3477)
Dr. Ilan Roth (part-time); <i>Research Physicist, Space Science Lab, UCB</i>	187M	Cory Hall	(642-1327)
Dr. Bruce Cohen	L630	LLNL	(422-9823)
Dr. A. Bruce Langdon	L472	LLNL	(422-5444)
Dr. William Nevins <i>Adjunct Lecturers, UCB; Physicists LLNL</i>	L630	LLNL	(422-7032)
Mr. Perry Gray <i>Senior Engineering Aide</i>	119ME	Cory Hall	(642-3528)
Mr. William Lawson			
Mr. Niels Otani			
Ms. Lou Ann Schwager <i>Research Assistants</i>	119MD	Cory Hall	(642-1297)
	119ME	Cory Hall	(642-3528)

June 30, 1985

DOE Contract DE-AS03-76-F00034-DE-AT03-76ETS3064

ONR Contract N00014-77-C-0578

Varian Gift

Hughes Aircraft Co. Gift

ELECTRONICS RESEARCH LABORATORY

University of California  
Berkeley, California 94720

## **SECTION I: PLASMA THEORY AND SIMULATION**

### **A. Oblique Electron Bernstein Wave Investigations Linear Response Limits**

**Wm. S. Lawson**

In studying these waves, obtaining limits to linear response was found to be very important. Hence, a simpler model was chosen. The results are being prepared as an ERL Memorandum (now ERL Memo M86/44, June 3, 1986) with title and abstract as follows:

#### **Limits of Linear Response of a Vlasov Distribution**

**by**

**William S. Lawson**

#### **Abstract**

The linear response of a spatially periodic Vlasov plasma distribution function is computed to second order in the electric field (this procedure is also given justification). The results for a specific electric field are then compared with the results of computer simulation for different amplitudes of the electric field. The onset of the deviations from linear theory as the amplitude increases are correctly predicted by trapping theory, indicating that trapping is responsible for limiting the validity of linear theory.

### **B. Simulation of the Effect of Large Amplitude RF-Waves on the Interchange Instability-Supporting Theory**

### **C. One-Beam Alfvén Ion-Cyclotron Instabilities of Multiple Ion Distribution Functions**

### **D. Linear Mode Coupling in Simulations of the Alfvén Ion-Cyclotron Instability**

**Niels F. Otani**

Final reports are in preparation in all of these areas, to be issued as ERL memoranda, to be sent out with the QPR's, when ready. The titles may be altered slightly from those above. One abstract follows.

### **E. Simulations of the Weak Warm-Beam-Plasma Instability: Study of the Correlation Functions**

**Dr. K. Theilhaber**

This is work begun by Dr. Theilhaber in France and completed here, to be issued in an ERL Memorandum, "Numerical Simulations of Turbulent Trapping in the Weak Beam-Plasma Instability," by K. Theilhaber, ERL Memo M86/50, June 5, 1986.

## **The Alfvén Ion-Cyclotron Instability: Simulation Theory and Techniques**

Niels F. Otani  
Electronics Research Laboratory  
University of California  
Berkeley, CA 94720

A particle-ion, fluid-electron computer simulation code is used in the study of the Alfvén ion-cyclotron (AIC) instability, a parallel-propagating electromagnetic instability driven by temperature anisotropy in the ion velocity distribution function. A numerical odd-even mode is suppressed by means of a two-timestep averaging method. Excellent energy conservation is obtained by using a method similar to the Boris particle mover to advance the transverse fields. Linear growth rates obtained from the code differ substantially from those predicted by uniform Vlasov theory, here derived using a multifluid model. Short wavelengths in particular show substantial growth rates when damping is predicted, and additionally show strong linear mode coupling. Positive growth rates are even observed in the case of a Maxwellian ion distribution. Disagreement is also generally found among short-wavelength mode frequencies. These inconsistencies are resolved by taking into consideration general grid and discrete-particle effects of the simulation model. A theoretical study reveals a real, physical process by which an ion distribution may collisionlessly relax via short-wavelength AIC instabilities acting resonantly on small portions of the distribution function. This process is combined with a linear mode coupling theory and other characteristics of the AIC instability to explain all observed differences. Nonlinear short-wavelength saturation levels are also obtained and their relevance to other field-aligned, electromagnetic simulations is discussed.

To be issued as ERL Memo M85/91, November 25, 1985

## SECTION II: PLASMA-WALL PHYSICS, THEORY AND SIMULATION

### A. Transport of Particle and Energy Fluxes through the Plasma-Sheath Region Including Ion Reflection

*Lou Ann Schwager*

#### I. Introduction

Ion reflection at a collector plate affects the ability of the sheath to thermally insulate the plate from the plasma. The atomic data for ion reflection and derivation of electrostatic potential drop through the sheath and of the kinetic energy flux to the plate is discussed in a previous report (QPR III,IV 1984). Through this analysis and detailed comparison to simulation using PDW1, we have found that, for a bounded system with a constant, injection flux, increasing the reflected ion current generates a potential which decreases the insulating effect of the sheath. For this study we use an ion to electron mass ratio of 40 and ion reflection coefficients of  $R=0$ , 20, and 40% with the same system model as before.

Our simulation of a bounded system with a constant injection source models the constant generation of ions and electrons by ionization in the central, collisional section of a plasma device. Consequently boundary effects, such as ion reflection, affect not only the plasma characteristics but also the actual, equilibrated density in the system. Thus for a system with constant, injected flux, the increase in ion reflection causes a buildup of plasma density which overall increases the kinetic energy flux to the plate.

#### II. Theory Review

In the previous report (QPR III,IV 1984) we describe the kinetic energy flux to the plate as the sum for all three plasma components of the energy carried per particle times the particle flux at the electrically insulated boundary. First let us consider the contribution of the electrons. In one dimension, on average each incident electron, with a mean speed of  $\langle v \rangle = (2kT/\pi m)^{1/2}$ , carries an energy of  $1kT$  to the plate by thermal effusion.<sup>1</sup> Kinetically

the mean speed of these Maxwellian electrons is defined by

$$\langle v \rangle \equiv (2\pi v_t^2)^{-1/2} \int_0^{\infty} v \exp\left(\frac{-v^2}{2v_t^2}\right) dv. \quad (1)$$

The density of electrons hitting the plate is one-half the density determined by the electrostatic potential through the Boltzmann equation:

$$n_{e0} = \frac{1}{2} n_{\infty} \exp\left(\frac{e\phi_0}{kT}\right). \quad (2)$$

A discussion of why the electrons carry an energy of  $1kT$  (in one-dimension) is presented in the appendix of the aforementioned report. Hence electrons with an energy

$$E_{e0} = kT \quad (3)$$

contribute a kinetic energy flux of

$$Q_{e0} = F_{e0} kT, \quad (4)$$

where the particle flux at the plate is

$$F_{e0} = \frac{1}{2} n_{\infty} \exp\left(\frac{e\phi_0}{kT}\right) \langle v \rangle. \quad (5)$$

Using the following definition, we can derive this relation for  $Q_{e0}$  in one-dimension with

$$Q_{e0} = n_{\infty} (2\pi v_t^2)^{-1/2} \int_0^{\infty} v^3 \exp\left(\frac{-v^2}{2v_t^2}\right) dv. \quad (6)$$

We next evaluate the contribution of the primary and reflected ions to the kinetic energy flux at the plate. Because we assume the plate is electrically insulated or floating, the electron flux  $F_{e0}$  equals the primary ion flux  $F_{i0}$  into the plate minus the reflected ion flux  $F_{r0}$  away from the plate. Using the definition of ion reflection coefficient,

$$R \equiv -F_{r0}/F_{i0}, \quad (7)$$

along with the open circuit condition, we find that

$$F_{i0} = F_{e0}/(1 - R) \quad (8)$$

and

$$F_{r0} = -RF_{e0}/(1 - R). \quad (9)$$

The primary ions carry their initial energy  $\mathcal{E}_{i\infty}$  on entering the sheath region plus that gained from the drop in potential of  $-e\phi_0$ . Thus each primary ion imparts to the plate a total energy  $\mathcal{E}_{i0}$  where

$$\mathcal{E}_{i0} = \mathcal{E}_{i\infty} - e\phi_0. \quad (10)$$

For simplicity we assume the plate absorbs no energy during reflection. \* Then the reflected ions remove the same energy as the primary ions add. As shown in the previous report (QPR III,IV 1984: Eq. (18)),  $\mathcal{E}_{i\infty} \geq kT/2$  for cold ions. With the injection of warm ions,  $T_i = T$ , these enter the sheath region with initial energy  $\mathcal{E}_{i\infty}$  equal to  $kT$ . With this assumption then the kinetic energy flux for primary ions is

$$Q_{i0} = \frac{F_{e0}kT}{1 - R} \left( 1 - \frac{e\phi_0}{kT} \right) \quad (11)$$

and for reflected ions is

$$Q_{r0} = \frac{-RF_{e0}kT}{1 - R} \left( 1 - \frac{e\phi_0}{kT} \right). \quad (12)$$

In an equilibrated system with a constant, injected flux and temperature, the electron flux incident to the plate must be equal to the injected flux  $F_{e\infty}$ . With the same  $F_{e0}$  for

---

\* Typically for a low temperature plasma, the wall absorbs about 20% of the incident particle energy. The specific fraction depends on the mass ratio of the incident particle and wall target.<sup>2</sup>

each variation in reflection coefficient  $R$ , we see that  $Q_{e0}$  is independent of  $R$  as is  $n_{e0}$ . Thus for the plate electron density of Eq. (2) to be independent of  $R$  (and  $\phi_0$ ) then  $n_\infty$  must be increasing. For the ions, net kinetic energy flux,  $Q_{i0} + Q_{r0}$ , depends directly on the floating plate potential. As we increase  $R$ , this drives up the magnitude of the potential  $\phi_0$  according to the previously derived relation (QPR III,IV 1984: Eq. (21)), which is

$$\frac{-e\phi_0}{kT} = \ln \left[ \left( \frac{1+R}{1-R} \right) \left( \frac{M}{2\pi m} \right)^{1/2} \right]. \quad (13)$$

Thus the net ion contribution rises slightly only because of the added energy that the ions gain in accelerating through a larger potential drop.

Instead of fixing the injected flux, suppose we hold  $n_\infty$  constant by appropriately lowering the injected fluxes as we increase  $R$ . Then the larger sheath drop will better insulate the plate from the hot electrons, i.e.  $Q_{e0}$  falls linearly with  $F_{e\infty}$ . With  $n_\infty$  fixed, ion kinetic energy flux falls because the exponential drop in plate density overshadows the small gain in incident ion energy.

The choice of whether to fix  $n_\infty$  or  $F_{e\infty}$  dramatically affects the dependence of  $Q_0$  on  $R$ . We show this difference in the two graphs of Fig. 1. The parameters used in the simulation and substituted into Eqs.(4) and (11)–(13) for Fig.1 are  $F_{e0} = 500$ ,  $M/m = 40$ , and  $e = kT = 0.05$ . Potential is calculated with Eq. (13). We believe that holding the injected flux constant, rather than  $n_\infty$ , better models a bounded plasma device. From this point forward all statements of trends will use the assumption that we fix the injected flux while varying  $R$ .

### III. Simulation Transport Diagnostics

Next we present how PDW1 evaluates the above plasma characteristics. Diagnostics for moments of the distribution function are evaluated as particles leave the bounded system within each time step. Usually at each time step we can extract the velocity of all

the particles weighted to a grid point. Distributing the particles according to velocity into many velocity bins of width  $\Delta v$  determines at that position and time the particle distribution,  $f(v)\Delta v$  particles in element  $\Delta v$ . As particles penetrate the plate, the simulation provides the velocity of each particle passing the last grid point per unit time, i.e. the flux distribution,  $v f(v)\Delta v$  particles in the element  $\Delta v$  per unit time  $\Delta t$ . For each passing particle, indexed with  $i$ , then  $v_i f_i(v)\Delta v = 1$ . If we let  $V_i = v_i f_i(v)\Delta v$ , then the particle flux, in numbers per  $\Delta t$ , hitting the plate is

$$F_0 = \sum_i V_i. \quad (14)$$

Similarly the effective density at the plate is

$$n_0 = \sum_i V_i / v_i. \quad (15)$$

Hence the mean speed of these particles is

$$\langle v \rangle = F_0 / n_0. \quad (16)$$

We calculate the average kinetic energy that a particle has at the plate with

$$\mathcal{E}_0 = \frac{m}{2n_0} \sum_i v_i V_i. \quad (17)$$

Finally the kinetic energy flux is determined with

$$Q_0 = \frac{m}{2} \sum_i v_i^2 V_i. \quad (18)$$

To reduce noise in these diagnostics, we evaluate the spatially-averaged plasma period and then average the above values over that plasma period.

#### IV. Simulation Set-up

We use the same model as that shown in the previous report (QPR III,IV 1984). Specifically the input used follows in Table 1.

Table 1. Simulation Set-Up

System Parameters	Injection Parameters
Initially Empty	Ion Flux=500.
Open External Circuit	Electron Flux=500.
Length=2.	Electron Thermal Velocity=1.
Grid Number=128	Ion Thermal Velocity=0.158
$\Delta t=3.906 \times 10^{-3}$	Electron Temperature=0.05
Particle Charge=0.05	Ion Temperature=0.05
Electron Mass=0.05	
Ion Mass=2.	

## V. Comparison of Theory and Simulation

To determine the theoretical values for kinetic energy flux, we inserted the potential calculated in the simulation into Eqs. (10)–(12). The magnitude of the plate potential measured from the simulation exceeds that predicted in Eq. (13) because the injected ions enter the system with  $T_i = T$  rather than  $T_i \ll T$ . The first results for each variable listed in Table 2 is that which theory predicts. The second result is output from PDW1. The range indicated for simulation results show the amplitude of oscillation. All values from simulation are measured after the total number of particles in the simulation is unchanging.

We present in Fig. 2 an example of the history of kinetic energy flux to the plate for both ion streams. Here  $R = 40\%$  for a flux history that spans the last fourth of the simulation in time. The small dip at  $time \approx 87$  occurs because the ion-ion two-stream instability causes the ion streams to interact and whirl. (See the previous report.) This results in an effective reduction in kinetic energy flux because of the drop in density from the ion hole created in phase space which hits the plate. Figure 3 shows the ion phase space profile at six times during the simulation.

## VI. Conclusions

All of the assumptions used in the derivation of the time-independent theory of kinetic energy flux to a boundary with ion reflection are verified by our simulation using

PDW1. Even with the onset of two-streaming, the average value of the transport results is unaffected.

We determine that the electrons do indeed carry an average energy of  $1kT$  to the plate as verified in Table 2 by the results for  $Q_{e0}$ . However with the diagnostic of average particle energy at the plate, we see that PDW1 consistently generates  $\mathcal{E}_{e0} \approx kT/2$  rather than  $kT$ . In addition PDW1 generates for all three cases an electron temperature profile that drops from  $kT$  at the source to  $kT/2$  at the plate. Thus the history of electron kinetic energy at the plate indicates that  $\mathcal{E}_{e0}$  equals the electron temperature measured at the plate. We point out in Table 2 that  $Q_{i0}$  is also accurately predicted. This verifies the assumption that the ion energy carried from the bulk plasma to the boundary is  $kT - e\phi_0$ . Again the value  $\mathcal{E}_{i0}$  specifically calculated by PDW1 is overpredicted by theory. If we use the computational results for  $\mathcal{E}_{i0}$  along with Eq. (11), then we find  $\mathcal{E}_{i\infty}$  is  $0.84 kT$  for  $R=0\%$  and  $0.88 kT$  for  $R=20\%$  and  $40\%$ . Consequently we ask the following question with the hope that in the near future we can answer it. Is the average energy that a particle carries from the bulk plasma to the boundary that same as the average kinetic energy that a particle has when hitting the plate?

#### Reference

- [1] J. H. Jeans, *The Dynamical Theory of Gases*, Dover Publications, New York, 1925, p.121.
- [2] R. A. Langley et al, "Data Compendium for Plasma-Surface Interactions", *Nuclear Fusion* special issue, (1984), pp.12-27.

# Theory and Simulation Results

Variable	Reference Eq. ( )	R	0%	20%	40%
$\frac{-e\phi_0}{kT}$	(13)		0.93	1.33	1.77
	-		$1.04 \pm 0.10$	$1.40 \pm 0.11$	$1.82 \pm 0.15$
$n_{e0}$	*		627	627	627
	(15)		$630 \pm 90$	$630 \pm 110$	$630 \pm 180$
$F_{e0}$	-		500	500	500
	(14)		$500 \pm 20$	$500 \pm 20$	$490 \pm 30$
$F_{r0}$	(9)		0	-125	-333
	(14)		0	$-125 \pm 7$	$-330 \pm 25$
$\mathcal{E}_{e0}$	(3)		0.05	0.05	0.05
	(17)		$0.026 \pm 0.004$	$0.025 \pm 0.005$	$0.025 \pm 0.005$
$\mathcal{E}_{i0}$	**		0.102	0.120	0.141
	(17)		$0.094 \pm 0.007$	$0.114 \pm 0.004$	$0.135 \pm 0.006$
$Q_{e0}$	(4)		25	25	25
	(18)		$25 \pm 1$	$25 \pm 1$	$25 \pm 2$
$Q_{i0}$	(11)		51	75	117
	(18)		$51 \pm 2$	$75 \pm 4$	$117 \pm 7$
$Q_{r0}$	(12)		0	-15	-47
	(18)		0	$-15 \pm 3$	$-47 \pm 5$

\*  $n_{e0} = F_{e0}(2kT/\pi m)^{-1/2}$  from Eqs. (2) and (5).

\*\* Use Eq. (10) with  $\mathcal{E}_{i\infty} = kT$ .

Table 2. Comparison of theory and simulation using the values presented in Table 1. The first value for each variable is that from theory; the second is from PDW1.

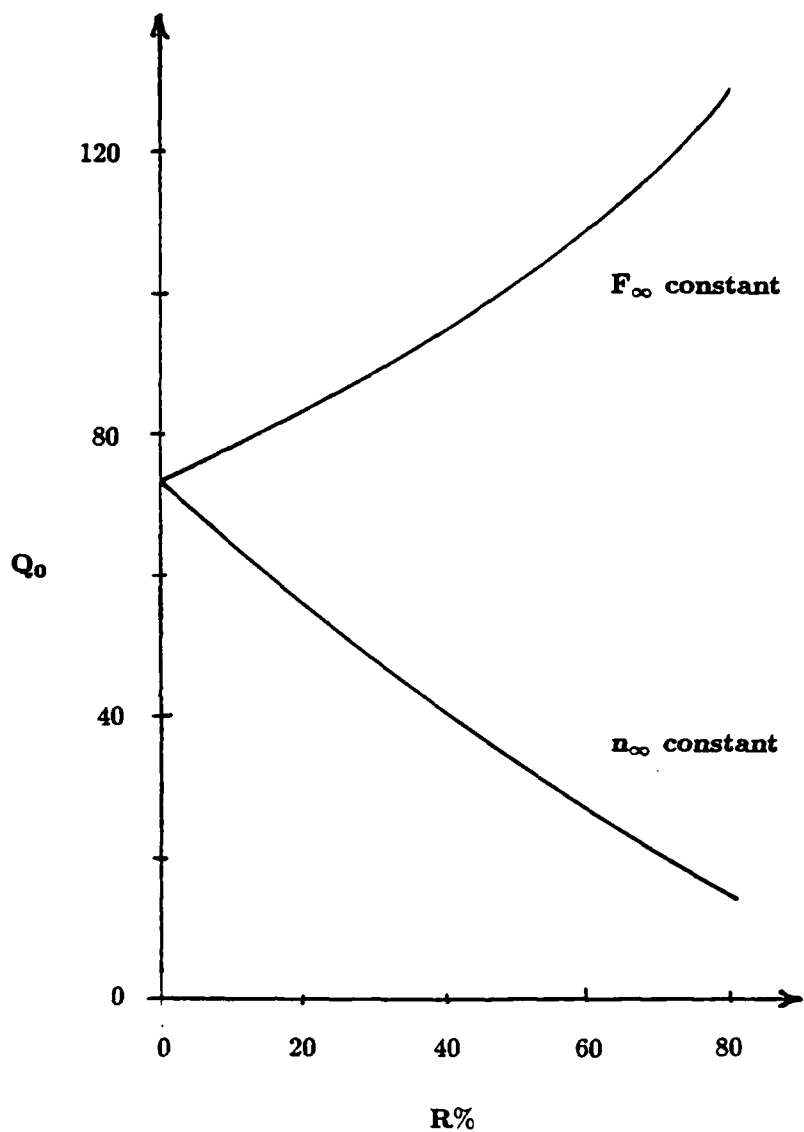


Figure 1. Dependence of the kinetic energy flux to a collector plate  $Q_0$  on ion reflection coefficient  $R$  for constant, injected fluxes  $F_\infty$  and constant background density  $n_\infty$ .

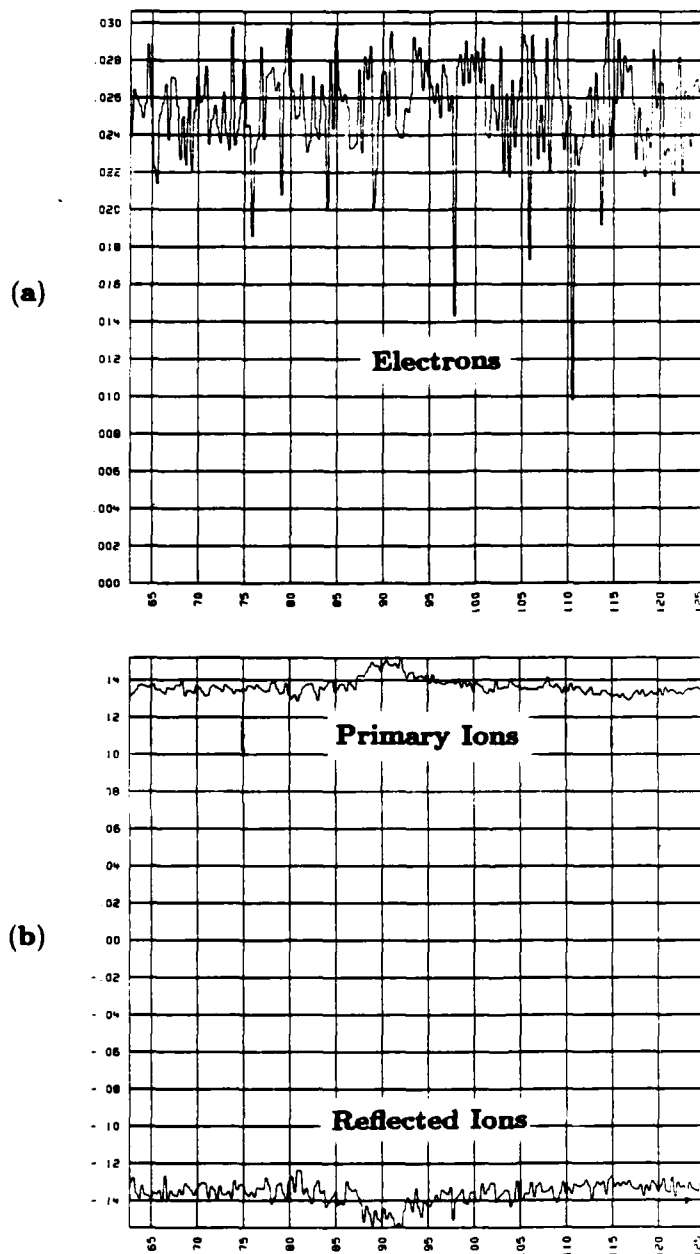


Figure 2. History of kinetic energy flux to the plate by (a) electrons and (b) primary ions and reflected ions for  $R=40\%$ . Time units in *step number*  $\times \Delta t$ . Shown in time is the last fourth of the simulation run.

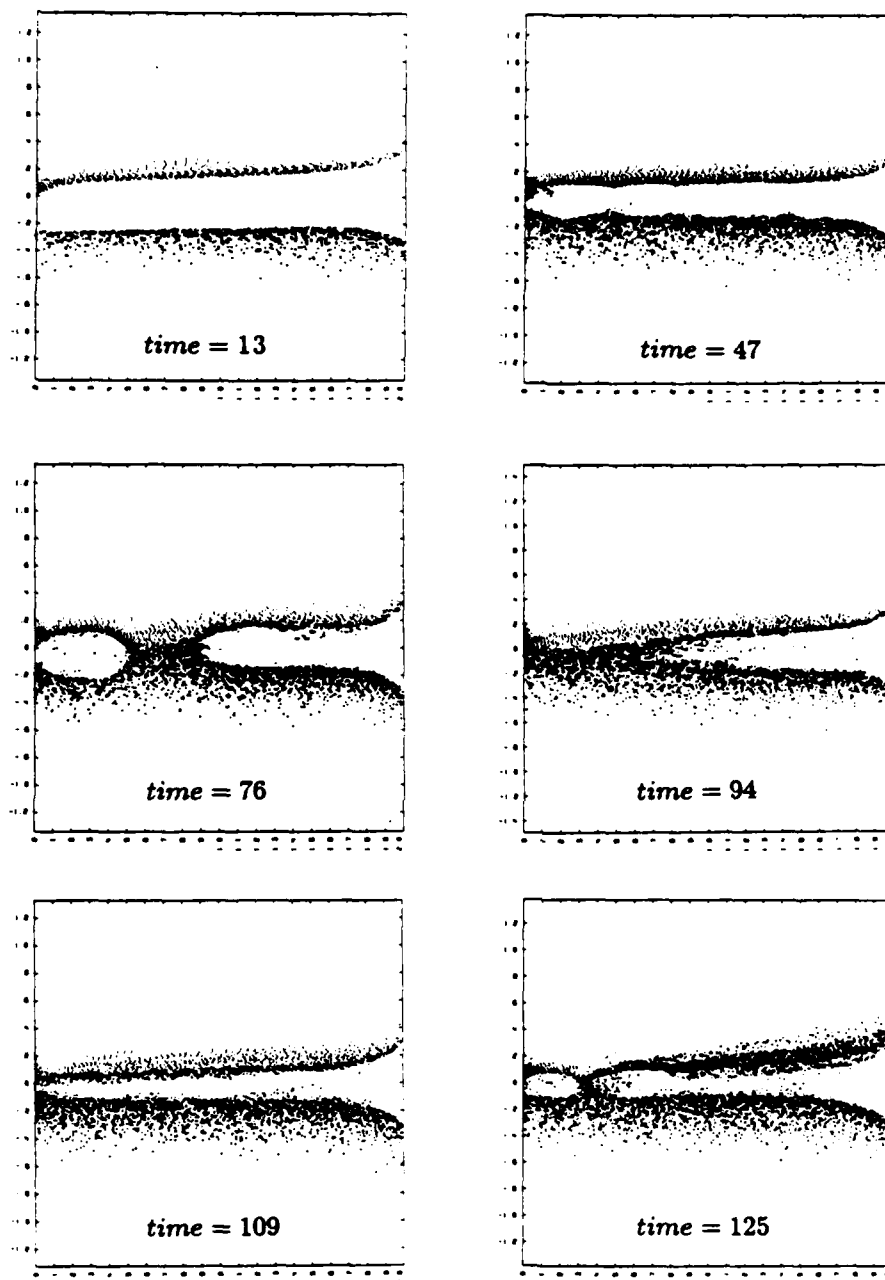


Figure 3. Profiles in ion phase space at various times for  $R=40\%$ . Source at  $x=0$ . Plate at  $x=2$ . Ion thermal velocity at  $x=0$  is 0.158. Primary ions are denoted by “.”; reflected ions by “+”.

## B. Planar Magnetron Discharges

Amy Wendt (Prof. M. A. Lieberman, Dr. Herman Meuth)  
Perry Gray (Prof. C. K. Birdsall)

### (1) Progress on Experimental Apparatus

Construction and testing of the experimental apparatus has been completed, and it is now in use. No major design changes from that already described in previous reports were necessary. Electrodes have been mounted on pistons which carry two teflon o-rings that seal the piston radially against a cylindrical outer chamber. A diffusion pump evacuates the main vacuum region, and a mechanical pump differentially pumps between the two seals on each piston. This prevents air from leaking into the main vacuum region when the pistons are moved during operation. This design has proven successful; the system has a base pressure of less than  $10^{-5}$  torr.

The electromagnet for planar magnetron operation of the experiment has been designed and built. The design was completed with the use of *POISSON*, a two dimensional magnet modelling code available to us through National Magnetic Fusion Energy Computing Center. Given the geometry of a magnet design, the code maps out magnetic field lines and contours of constant magnetic field. This allowed us to choose a configuration of magnetic windings and iron core which would fit the space available and which would optimize the mirroring of electrons in the magnetic field. In order to retain some flexibility in the geometry of the magnetic field, removable pole pieces were used on the iron core which may be replaced by pole pieces of different shapes. The magnet has been wound and tests have been made of the water cooling and electrical systems. The magnet is now set up on a workbench so that its magnetic field can be measured. A poor man's optical bench has been devised so that a gauss-meter can be used to make spatially resolved measurements of radial and azimuthal fields.  $B_r$  was measured as a function of  $r$  for various values of  $z$  with results very similar to Fig. 3 in QPR 3 and 4 1984, page 53;  $B_r \approx 1000$  gauss at the cathode plate was obtained for magnet current of 2900 A. The magnet will be installed as soon as testing is completed.

At the same time, work has been done on characterizing the dc glow discharge. The automatic pressure control system has been set up and works well. Several Langmuir probes have been made and are mounted on the diagnostic ports. The probes have sliding seals so the radial position of the probes can be varied. A single Langmuir probe has been made out of 0.005 in. diameter platinum wire encased in alumina tubing with a 0.014 in. sphere exposed to the plasma. The spherical probe tip was made by heating the end of the platinum wire with a torch. Two double probes have also been made. The two probes which make up the double probe are biased with respect to each other but float with respect to the chamber. One of the double probes was made with platinum wires exactly as described above for the single probe. The other double probe was made using a pair of paralleled platinum disks 0.313 in. in diameter. The back sides of the discs were coated with epoxy resin so that they are nonconductive. The increased area of this double probe allows for an increased probe current so that measurements can be made even at low density. Circuitry is available to evaluate the probe current-voltage characteristic, using either a dc bias for point-to-point measurement or a swept bias for continuous measurement. The probe has been used to measure electron density in the glow discharge and will also be used for measuring the electron temperature.

We have also studied the current-voltage characteristic of the discharge at various pressures. We have observed that the current drawn from our constant voltage supply has a tendency to be unsteady both on a short time scale (corresponding to flashes of light from the discharge) and on a longer time scale (slow drifts of both increasing and decreasing current). To remedy this problem, we are increasing the voltage dropping resistors which are in series with the glow discharge so that effectively the discharge will see a constant current supply.

### (2) Modelling and Simulation

The simulation model we are working with for the planar magnetron has been described in Figure 6 page 56 in the previous QPR (3 and 4, 1984). We are currently implementing modelling of

ionization by volume creation of electron-ion pairs with provisions to make this a function of local variables (e.g., local density), allowing the magnetic field to vary with distance from the cathode, and inserting additional transport diagnostics.

Electron-neutral collisions are modelled with electrons scattering off a fixed background of neutrals as if hard and massive spheres (elastic collisions). At a given time step, the number of collisions that occur is determined through an inverse cumulative Poisson distribution so as to be random in time, about a given mean value. Then particles to be scattered are chosen randomly from the particle population; a particle may be scattered more than once in a given time step. Scattering angles are chosen using the cosine probability for hard sphere collisions and the phase angle is chosen uniformly randomly in the interval 0 to  $2\pi$ . The computer routines to model collisions in this manner have been written and are being tested to see whether they produce the expected statistics for the angular spread in time of an initially mono-energetic distribution of ballistic particles (a beam). The free parameter for this model is the density of the background neutrals. This model does not properly handle energy exchange between species or ionization and excitation of neutrals. However, we believe it is a good first step for the effect of collisions on the plasma behavior in the regime where electron-neutral collisions exceed Coulomb collisions.

### C. Particle Simulations of the Low $\alpha$ Pierce Diode

*T. L. Crystal, S. Kuhn*

This work was completed with publication of an article with the above title and authors in *Physics of Fluid*, 28, pp. 2116-2124, July 1985.

### D. Thermionic Emission I-V Knee Paradox

Perry Gray, Wm. S. Lawson (Prof. C. K. Birdsall)

(1) *Introduction.* Electron emission current density in a planar diode with a hot dispenser cathode (thermionic emission) is supposedly well known. However, R. T. Longo<sup>1</sup> proposed that the net current density from a hot cathode was a particular mixture of space-charge and temperature limited values. He proposed the empirical fit

$$\frac{1}{J_{\text{total}}} = \frac{1}{J_{\text{space charge limited}}} + \frac{1}{J_{\text{temperature limited}}} \quad (1)$$

where the space-charge limited current density is the usual Child's Law (1911)

$$J_{\text{SC}} = K_1 V^{3/2} / d^2 \quad (2)$$

and the temperature-limited current density is the usual Schottky Law (1914)

$$J_{\text{TL}} = J_{\text{sat}} \exp \left( K_2 \sqrt{\frac{V}{d}} / T \right) \quad (3)$$

where  $V$  is the anode voltage and  $d$  is the cathode-anode spacing. Longo<sup>2</sup> showed remarkable agreement, reproduced here as Figure 1, with Eq. (1), with no sharp knee juncture of Eqs. (2, 3); he labels this as "Langmuir Theory" (perhaps a trifle unfair).

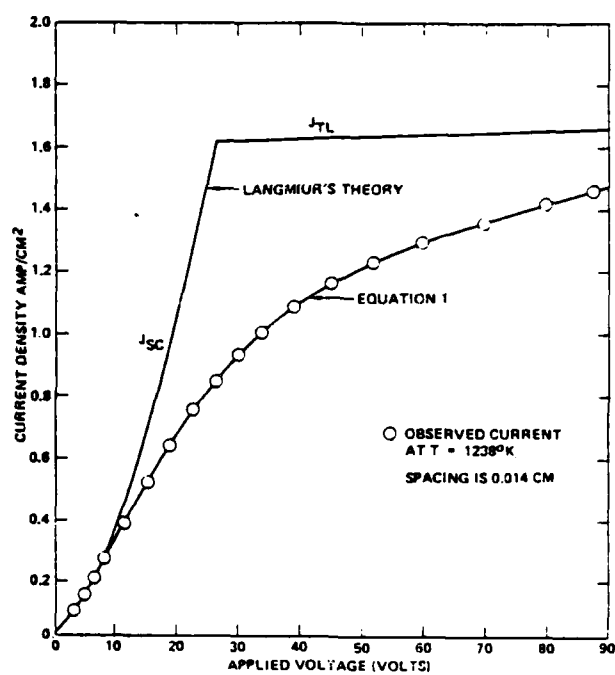


Figure 1 Dispenser cathode data, taken in a close space diode, evaluated with Langmuir's theory and Equation 1.

Longo found formula (1) to hold at different diode spacings and at different temperatures. His colleague, E. A. Adler, has looked at the effect of work-function nonuniformities (patchiness) and found analytically<sup>3</sup> that the motion of particles in two dimensions tends to average out the effects of patchiness having length scales that are large compared with  $\lambda_D$ . Patchiness effects were also measured experimentally (Longo, Adler, Harrison, and Sundquist<sup>4</sup>), using a 0.005" sampling hole in the anode scanned across a single crystal LaB<sub>6</sub> cathode, finding average work function variation of 0.001 eV (tiny) over an average path length  $< 8 \mu$ ; the conclusion was that the deviation (smooth not sharp knee) cannot be entirely understood by patch effect. Adler and Longo<sup>5</sup> state that noise in the emitted current and in the space charge can also result in a smoothing of the transition between the two regimes of the diode; they emphasize that the diode is a nonlinear device, very strongly so at the transition, so that it is quite possible that noise can affect the time-average current.

(2) Relation to work here. Our group has been active in bounded plasma theory and simulation, especially in studying the plasma sheath since 1981. The electron emitter (not a plasma, no ions), in some sense, is a version of the sheath, it may have complicated phase space and appreciable fluctuations, is capable of rectifying, and so on. Hence, it is quite natural to study the time-dependent electron emitter (a "non-neutral plasma") along with plasma sheaths. It is even advantageous to do so, as past excursions have lead to useful inventions. (Our noise studies in 1959 lead to virtual cathode oscillations (see Birdsall and Bridges<sup>6</sup>) which now are called vircators, producing immense microwave and millimeter wave powers.) The Hughes group has provided considerable insight into the "smooth knee" problem and stimulated us to look into the role of fluctuations in producing the smooth knee, which we are now starting.

(3) Past work here. The closest past work here is that of S. Rousset<sup>7</sup> with the Child-Langmuir diode. His cool injection short-circuit diode results (Figs. 27, 28 for constant injection) show nearly constant anode current ( $J \approx 40$ ) but very large periodic bursts of current returning to the cathode (like relaxation oscillations) and non-simple motion of the potential minimum in space (versus time). His warm injection diode results (Figs. 29, 30), however, show almost no oscillations in any component of the current ( $J \approx 60$ ) and more clearly steady potential minimum. (These are also like the cold and warm virtual cathode oscillations of Ref. 6.) The sole difference is the temperature of the injected particles; the emitted number/second is the same. These differences in current appear to be in the direction of the effect being sought, but with no applied potential.

(4) Current work. We need to be more quantitative with a model like Rousset's, looking at noise and at internal bursts and oscillations. Rousset modified our periodic code ES1 to allow for non-neutral charge density, using an inversion technique. We will use our bounded code PDW1 for the same purposes.

#### REFERENCES

1. R. T. Longo, "Long life, high current density cathodes," *Technical Digest, International Electron Devices Meeting*, December 1978, pp. 152-158.
2. R. T. Longo, "A study of thermionic emitters in the regime of practical operation," *Technical Digest, International Electron Devices Meeting*, December 1980, pp. 467-470.
3. E. A. Adler, "Effect of nonuniform work function on space charge limited current," poster paper APS/DPP Meeting, Boston, 1984.
4. R. T. Longo, E. A. Adler, C. R. Harrison, and W. F. Sundquist, "Experimental test of the space-charge to saturated transition in thermionic diodes," poster paper APS/DPP, New Orleans, 1982.
5. E. A. Adler and R. T. Longo, "Effect of noise on current in a thermionic diode," Tri-Services Cathode Workshop, NRL, Washington, D.C., April 1984.
6. C. K. Birdsall and W. B. Bridges, *Electron Dynamics of Diode Regions*, Academic Press, NY (1966). See Chapter 3.
7. S. Rousset, "Time-dependent Child-Langmuir diode simulation," UCB/ERL Memo M83/39, 11 July 1983.

### SECTION III: CODE DEVELOPMENT AND SOFTWARE DISTRIBUTION

Codes which we have developed or modified here are, generally speaking, available for the asking. We are making arrangements with our Industrial Liaison Program to handle distribution, at cost, of listings, tapes and/or diskettes. In a later report we will provide a list of codes and related material available and how to obtain such. If you use those, we simply ask that you acknowledge the source and also send us your results as published in reports or journals.

(Not all of the codes mentioned in our reports are available for distribution; some are single-purpose, single-user, too stylized for outside use.)

#### A. POLY: A Hybrid Scheme for the Solution of the Vlasov Equation

*K. Theilhaber*

##### I. INTRODUCTION.

In this report, we present a hybrid numerical scheme for the simulation of plasmas where one component can be modelled by linearized fluid equations, the remainder of the plasma being described by the full Vlasov equation. For both plasma components, numerical solutions are obtained through finite-difference methods.

For instance, the hybrid scheme is well adapted to the study of the initial phases of the weak warm beam instability, where a weak beam interacts with a massive bulk plasma. In this situation, it is essential to retain all of the phase-space dynamics of the beam. On the other hand, the bulk plasma merely sustains plasma oscillations, and it is appropriate to model it as a linear fluid, thereby saving a very considerable amount of mesh size and computational time.

In what follows, we shall present normalized equations for the beam-plasma problem, and then sketch our methods of solution. It should be kept in mind that the formulation of the problem can be generalized in a straightforward fashion: thus, the "beam" can just as well represent a warm but stationary plasma, and its density need not be small compared to the density of the bulk plasma; the model for the bulk plasma can be modified, so as to include thermal dispersion or damping, effects which we are ignoring in the present formulation of the scheme.

##### II. THE PHYSICAL PROBLEM AND ITS NORMALIZATIONS.

Our plasma is one-dimensional and consists of one species, electrons moving against an immobile neutralizing background of ions. A qualitative sketch of the initial, unperturbed distribution function is shown in Fig.(1), in which the curve representing the bulk should be thought of as a very narrow, cold beam at  $v = 0$ . Because our code is aimed at exploring the initial turbulence created in the beam-plasma instability, we can think of the beam distribution function as a tunable source of free energy.

Let the total, averaged spatial density of the electrons be  $n_0$ , with this density split between the bulk,  $n_{0P}$ , and the beam,  $n_{0B}$ ,  $n_{0P} + n_{0B} = n_0$ . In

the weak warm beam instability, the beam is a small perturbation to the bulk so that  $n_{0B} \ll n_{0P}$ , but this condition is not assumed in the numerical scheme.

We model the bulk evolution by the coupled linearized continuity and momentum equations:

$$\frac{\partial}{\partial t} \tilde{n}_P = -n_{0P} \frac{\partial}{\partial x} \tilde{u}_P, \quad (1)$$

$$\frac{\partial}{\partial t} \tilde{u}_P = \frac{q}{m} E(x, t) \quad (2)$$

where  $\tilde{n}_P$  and  $\tilde{u}_P$  are the linearized fluid variables. It is straightforward to add thermal dispersion or damping terms to these equations, but for simplicity we shall keep the bulk plasma as cold and collisionless.

The beam is described by a distribution function,  $f_B(x, v, t)$  which evolves according to the Vlasov equation:

$$\frac{\partial}{\partial t} f_B + v \frac{\partial}{\partial x} f_B + \frac{q}{m} \frac{\partial}{\partial v} f_B = 0, \quad (3)$$

with the normalisation of the unperturbed distribution function:

$$\int_{-\infty}^{\infty} dv f_B(v) = n_{0B}, \quad (4)$$

The electric field  $E(x, t)$  is determined self-consistently from Poisson's equation:

$$\frac{\partial}{\partial x} E(x, t) = \frac{q}{\epsilon_0} \left[ n_{0P} + \tilde{n}_B(x, t) + \int dv f_B(x, v, t) - n_{00} \right], \quad (5)$$

where we have subtracted from the electron-charge source terms the neutralizing charge of the immobile background ions.

We proceed to normalize eqs.(1- 5). We already have a characteristic time-scale, determined by the plasma frequency:

$$\omega_P^2 = \frac{q^2 n_0}{m \epsilon_0}, \quad (6)$$

but, because the bulk is cold, we cannot choose its thermal velocity as a reference velocity, nor the Debye length  $\lambda_D \equiv v_T/\omega_P$  as a reference length. Rather, we introduce a reference velocity  $v_R$  which will remain arbitrary for the moment, but which eventually will be tied to the width of the beam. The reference length is then  $\lambda \equiv v_R/\omega_P$ , and we define the normalized variables as:

$$t' = \omega_P t, \quad (7)$$

$$x' = x / \lambda_R, \quad (8)$$

$$v' = v / v_R. \quad (9)$$

$$E' = \frac{qE}{m\omega_P v_R}, \quad (10)$$

$$u'_P = \tilde{u}_P / v_R, \quad (11)$$

$$n'_P = \tilde{n}_P / n_{0P}, \quad (12)$$

$$f' = \frac{v_R}{n_{0B}} f_B. \quad (13)$$

Eqs.(1- 5) then become:

$$\frac{\partial}{\partial t'} n'_P = - \frac{\partial}{\partial x'} u'_P, \quad (14)$$

$$\frac{\partial}{\partial t'} u'_P = E'. \quad (15)$$

$$\frac{\partial}{\partial t'} f' + v' \frac{\partial}{\partial t'} f' + E' \frac{\partial}{\partial v'} f' = 0, \quad (16)$$

$$\int dv' f'_0(v') = 1. \quad (17)$$

$$\frac{\partial}{\partial x'} E' = R_P n'_P + R_B \left( \int f' dv - 1 \right). \quad (18)$$

where we have defined the important parameters,

$$R_B = \frac{n_{0B}}{n_0}, \quad (19)$$

$$R_P = \frac{n_{0P}}{n_0}. \quad (20)$$

which gauge the relative bulk and beam densities, the total density being normalized to 1, with  $R_P + R_B = 1$ . For convenience, we shall drop all primes in referring to the normalized equations.

For eqs.(14- 18), we can define the normalized energies of the electric field, of the bulk plasma and of the beam plasma particles. These are, respectively:

$$w_E = \frac{1}{2} \int E^2(x, t) dx, \quad (21)$$

$$w_P = \frac{1}{2} R_P \int u_P^2(x, t) dx, \quad (22)$$

$$w_B = \frac{1}{2} R_M \int \int v^2 f(x, v, t) dx dv. \quad (23)$$

and with these definitions, conservation of the total energy of the system follows:

$$\frac{d}{dt} w_{TOT} = \frac{d}{dt} (w_E + w_P + w_B) = 0, \quad (24)$$

### III. BOUNDARY CONDITIONS.

The variables  $\tilde{n}_P$  and  $\tilde{u}_P$  are defined on the one dimensional spatial mesh  $x_i = (i - 1)\Delta x, i = 1, 2, 3, \dots, N_X$ . The beam distribution function  $f(x, v, t)$  requires of course an additional mesh in  $v$ -space,  $v_j = v_{\min} + (j - 1)\Delta v, j = 1, 2, 3, \dots, N_V$ , where  $v_{N_V} = v_{\max}$ , and  $f$  is defined on the  $N_X \times N_V$  two-dimensional mesh. The spatial boundary conditions are chosen to be periodic, while in  $v$ -space we require the distribution function to be zero at the extreme boundaries,  $v = v_{\min}$  and  $v = v_{\max}$ . This latter requirement is not physical to the extent that the distribution function should really extend to arbitrarily large velocities. In operation, the Vlasov solver will tend to transport some density beyond the maximum velocity bounds, and in so doing will "forget" the profile of what was lost to higher velocities, resulting in a density (and energy) loss over time. However, by choosing  $v_{\min}$  and  $v_{\max}$  somewhat larger than the beam width and thus insuring that  $f$  is very small at the boundaries, these losses can be made extremely small, thus insuring consistency of the assumption of strictly zero density at the edges. The exceptions are those when very strong trapping occurs, in which case the trapping widths may extend to beyond the boundaries and density lost to high velocities.

#### IV. THE POISSON SOLVER.

We solve Poisson's equation:

$$\frac{\partial}{\partial x} E = n, \quad (25)$$

in two steps, through a potential  $\phi$ :

$$\frac{\partial^2}{\partial x^2} \phi = -n, \quad (26)$$

$$E = -\frac{\partial}{\partial x} \phi. \quad (27)$$

with the finite-difference form of these equations:

$$\phi_{i+1} - 2\phi_i + \phi_{i-1} = -\Delta x^2 n_i \quad (28)$$

$$E_i = -\frac{1}{2\Delta x} (\phi_{i+1} - \phi_{i-1}) \quad (29)$$

With a Fast Fourier Transformation, the solution for  $E$  is:

$$E(k) = -i \frac{\Delta x}{2} \cot \left( \frac{k\Delta x}{2} \right) n(k), \quad (30)$$

where  $k$  is the discrete wave-vector.

#### V. PUSHING THE BULK PLASMA.

In advancing eqs.(14-15), we use a finite-difference scheme of the "leapfrog" type, with the density defined at the same time as the electric field, and the velocity at  $\pm\Delta t/2$  time intervals before and after. Dropping the  $P$  subscripts on the variables, we have:

$$n_i^{(n+1/2)} - n_i^{(n-1/2)} = -\frac{\Delta t}{2\Delta x} (u_{i+1}^{(n)} - u_{i-1}^{(n)}), \quad (31)$$

$$u_i^{(n+1)} - u_i^{(n)} = \Delta t E_i^{(n+1/2)}. \quad (32)$$

where the superscripts indicate the time positioning. We solve eqs.(31) and (32) in Fourier space, with the FFT equations:

$$n^{(n+1/2)}(k) - n^{(n-1/2)}(k) = -i \frac{\Delta t}{\Delta x} \sin(k\Delta x) u^{(n)}(k), \quad (33)$$

$$u^{(n+1)}(k) - u^{(n)}(k) = \Delta t E^{(n+1/2)}(k). \quad (34)$$

While we have assumed so far that the bulk plasma is perfectly cold, the inclusion of a thermal dispersion term in eqs.(33- 34) should be straightforward, and will be attempted in future work. The overall accuracy of eqs.(33- 34) is  $O(\Delta t^2, \Delta x^2)$ .

## VI. PUSHING THE BEAM PLASMA.

The beam plasma distribution function is evolved synchronously with the bulk equations (31- 32), using a split-step method (C.Z. Cheng and G. Knorr) which involves transport in only one dimension,  $x$  or  $v$ , at a time. Had we a perfect one-dimensional transport scheme, the code would proceed as follows:

$$f^{(n+1/2)}(x, v) = f^{(n)}(x - v\Delta t, v), \quad (35)$$

$$f^{(n+1)}(x, v) = f^{(n+1/2)}(x, v - E^{(n+1/2)}(x)\Delta t). \quad (36)$$

where  $E^{(n+1/2)}(x)$  is determined self-consistently with the bulk and beam densities  $n_p^{(n+1/2)}$  and  $f^{(n+1/2)}(x, v)$ . Such a procedure can be shown to be accurate to order  $O(\Delta t^2)$ , the main difficulty residing in finding a comparably accurate transport scheme. Such a scheme is the "flux-corrected transport" (FCT) of Boris and Book<sup>(1)</sup>, which incorporates exceptionally low diffusivity over a large number of time steps.

We shall not describe the FCT scheme in detail, but note the salient features of the version used here. At the heart of FCT is a "smart", nonlinear filter which is interposed between a diffusive and an antidiffusive step. The nonlinear filter recognizes which features of the transported function have to be diffused for numerical stability, but preserves to the maximum extent physically meaningful features such as shock fronts. Because of this, FCT is well adapted to the "mixing" character of the Vlasov equation, where regions of different densities may coexist on short space and velocity scales.

In the terminology of <sup>(1)</sup> we are using a "low phase error", explicit, "phenical" FCT scheme, which solves the one-dimensional transport equation:

$$\frac{\partial}{\partial t} \rho + V \frac{\partial}{\partial \xi} \rho = 0, \quad (37)$$

In the notation of <sup>(1)</sup>, the diffusion and antidiffusion coefficients are, respectively:

$$\nu = \frac{1}{6} + \frac{1}{3}\epsilon^2, \quad (38)$$

$$\mu = \frac{1}{6} - \frac{1}{6}\epsilon^2. \quad (39)$$

where  $\epsilon \equiv V\Delta t/\Delta\xi$  measures the displacement at each time step relative to a mesh size. Transport in  $x$  and  $v$  are not handled in exactly the same way, as in the first case periodic and in the latter zero-value boundary conditions are imposed. In particular, as discussed in Section III, some particle loss to the edges in velocity space is inevitable but can be made very small.

## VII. ENERGY CONSERVATION.

In the absence of the beam plasma, the bulk equations (31-32), coupled to Poisson's equation (30), have an exactly conserved quantity which reduces to the sum of kinetic and electric-field energies in the limit  $\Delta x, \Delta t \rightarrow 0$ . If we define all quantities at the  $(n+1/2)$  time-step, then the electric-field energy is:

$$w_E^{(n+1/2)} = \frac{1}{2} \sum_{i=1}^{N_X} \left( E_i^{(n+1/2)} \right)^2 \cdot \Delta x, \quad (40)$$

and the corresponding bulk kinetic energy is:

$$w_P^{(n+1/2)} = \frac{1}{2} R_P \sum_{i=1}^{N_X} \left( u_i^{(n+1)} u_i^{(n)} - \frac{1}{4} (u_{i+1}^{(n+1)} - u_i^{(n+1)}) \cdot (u_{i+1}^{(n)} - u_i^{(n)}) \right) \cdot \Delta x \quad (41)$$

The second term in the sum, which vanishes as  $\Delta x \rightarrow 0$ , is a numerical "pressure" term, which arises from numerical dispersion. Thus, when  $R_P = 1$  and  $R_B = 0$ , the quantity

$$w_{TOT}^{(n+1/2)} = w_E^{(n+1/2)} + w_P^{(n+1/2)} \quad (42)$$

is exactly conserved during the plasma oscillations of the bulk.

On the other hand, while FCT conserves the integrated density exactly, it conserves energy only to  $O(\Delta t^2)$ . As the split-step transport scheme is itself only  $O(\Delta t^2)$  accurate, this is not a serious limitation. To  $O(\Delta t^2)$ , the beam kinetic energy is at the  $(n+1/2)$  time step:

$$w_B^{(n+1/2)} = \frac{1}{4} \sum_{i=1}^{N_X} \sum_{j=1}^{N_V} v_j^2 (f_{ij}^{(n+1)} + f_{ij}^{(n)}) \cdot \Delta x \Delta v \quad (43)$$

and with  $R_B \neq 0$ , the quantity:

$$w_{\text{TOT}}^{(n+1/2)} = w_E^{(n+1/2)} + w_P^{(n+1/2)} + w_B^{(n+1/2)} \quad (44)$$

is conserved to  $O(\Delta t^2)$  at each time step. These quantities correspond to the continuum quantities of eqs.(21- 23), and eq.(44) to the exact, physical energy conservation relation (24).

### VIII. LANDAU DAMPING ON A MAXWELLIAN.

For the initial testing of the code, and to motivate the rational development of its diagnostics, we considered a series of small-amplitude numerical experiments in which the accuracy of the integration scheme could be confronted, at least in the domain of linear theory.

We started with a series of experiments on linear Landau damping, for which we ignored the bulk package by setting  $R_P = 0$ , and for which the "beam" was no longer a beam, but a Maxwellian centered at  $v = 0$ . For these experiments, the initial, unperturbed distribution function is given by:

$$f_0(v) = \frac{1}{(2\pi)^{1/2} \Delta v_b} \exp(-v^2/2\Delta v_b^2) \quad (45)$$

and we considered the decay of a small, initial perturbation:

$$f(x, v, t = 0) = f_0(v) \cdot (1 + b \cos k_b x) \quad (46)$$

where  $b \ll 1$ . Note that in our normalized system, where  $\omega_P = 1$ , the Debye length for this thermal plasma is simply  $\Delta v_b$ . Starting from (46), an exact analytic solution of the linearised Vlasov-Poisson system yields:

$$E(x, t) = \frac{b}{k_b} \sin(k_b x) \cos(\omega_R t) e^{-\gamma t} + \text{Re} \frac{b}{i k_b} e^{i k_b x} \int \frac{f_0(v) e^{-i k_b v t}}{\epsilon(k_b, k_b v)} dv, \quad (47)$$

where  $\omega = \omega_R + i\gamma$  is the exact solution of the plasma dispersion relation:

$$\epsilon(k, \omega) = 1 + \frac{1}{k} \int \frac{\partial_v f_0}{\omega - kv} dv = 0, \quad (48)$$

which, for the Maxwellian distribution function becomes:

$$1 + \frac{1}{k^2 \Delta v_b^2} (1 + \zeta Z(\zeta)) = 0, \quad (49)$$

where  $\zeta = \omega/\sqrt{2}k\Delta v_b$ . In deriving eq.(47), we did assume that  $\omega_R/k_b \gg \Delta v_b$ . The first term in (47) is the linear fluid response of the plasma, with in addition a

Landau damping term  $\exp(-\gamma t)$ . The second term is the ballistic contribution, which for the Maxwellian  $f_0(v)$  decays as:

$$\exp(-t^2/t_{PM}^2), \quad (50)$$

where the phase-mixing time  $t_{PM}$  is given by:

$$t_{PM} = \frac{\sqrt{2}}{k_b \Delta v_b}, \quad (51)$$

For instance, we analysed the time-evolution of the electric field energy with the initial amplitude  $b = 0.001$ . For  $t \geq t_{PM}$  we should have:

$$w_E(t) = w_E(0) e^{-2\gamma t} \cos^2(\omega_R t), \quad (52)$$

and thus an analysis of the curve of  $w_E(t)$  can yield the numerical values of  $\omega_R$  and  $\gamma$ . An artisanal but reliable technique was used: the real part of the frequency was found by measuring, by hand, the spacing of the zeros of the field energy, while the damping was found from the decay of the envelope of the curve, also measured by hand. In fig.(2), the results of several runs are compared to the exact solution of eq.(49), obtained through Newton's method. The agreement is quite good. As an aside, we should note that the traditional electron-plasma dispersion relations:

$$\omega = 1 + \frac{3}{2} k_b^2 \Delta v_b^2, \quad (53)$$

$$\gamma = \left(\frac{\pi}{8}\right) \zeta^3 e^{-\zeta^2}, \quad \zeta = \frac{\omega}{\sqrt{2} k_b \Delta v_b}, \quad (54)$$

is of limited validity,  $k_b \Delta v_b \leq 0.1$ .

## IX. CONCLUSION.

The predictions of the hybrid code POLY have been checked in the case of Landau damping, a nontrivial linear phenomenon. Furthermore, in connection with the study of beam-plasma turbulence (the "turbulent trapping model"), we have been able to verify that the code yields results for small-scale, nonlinear plasma behavior which are consistent with the analytic models. We are thus gaining confidence that POLY is a robust numerical tool, which should have a wide applicability in situations where detailed dynamics are required for only a limited region of phase space.

## References

- <sup>1</sup> J.P.Boris and D.L.Book, in *Methods in Computational Physics*, J.Killeen ed., Academic Press, 1976, New York.
- <sup>2</sup> C.Z.Cheng and G.Knorr, *J. of Comp. Physics*, **22**, 330-351 (1976).

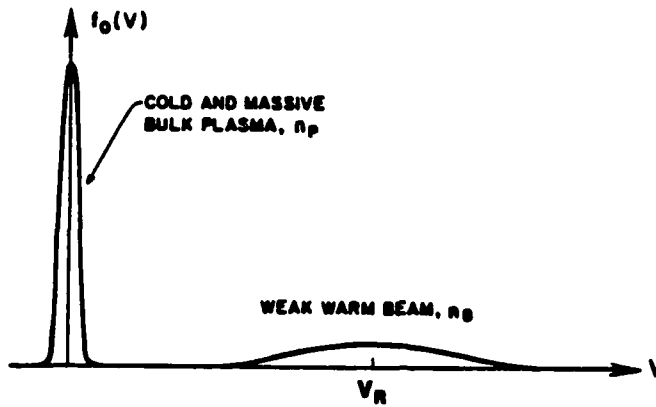


Fig. 1 : Initial distribution function for the beam-plasma instability.

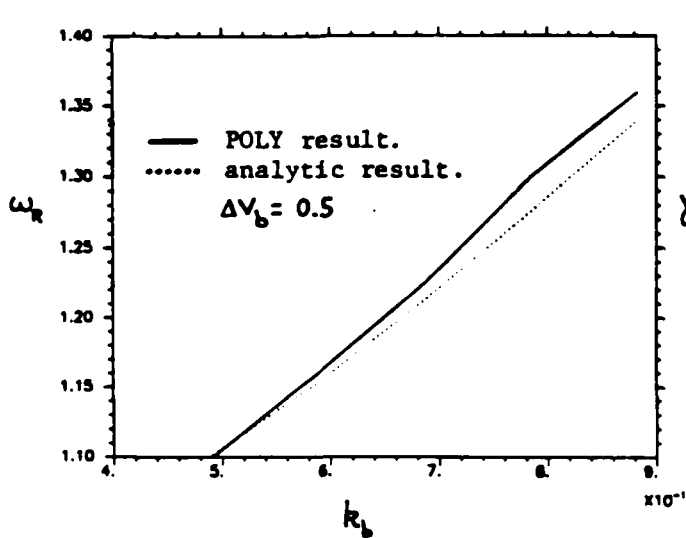


Fig. 2a : Comparison of results for the real part of the frequency for linear plasma waves.

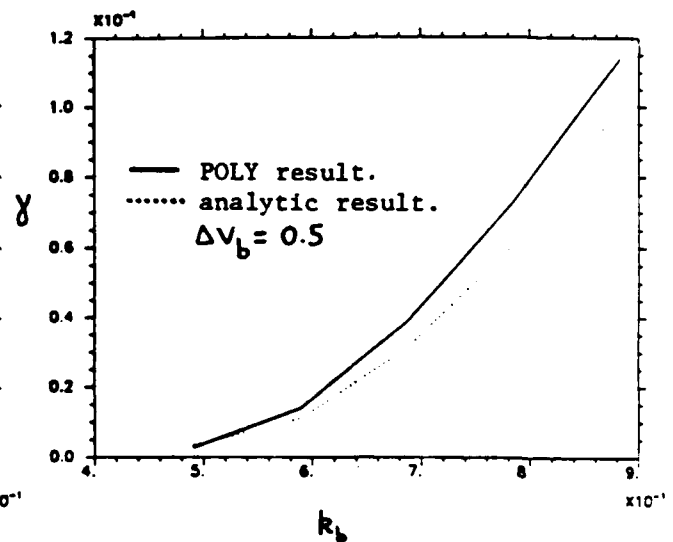


Fig. 2b : Comparison of results for the damping rate of linear plasma waves.

#### SECTION IV: JOURNAL ARTICLES, REPORTS, TALKS, VISITS

##### Journal Articles

V. A. Thomas, W. M. Nevins, "Electrostatic ion-ion two-streaming instability in a thermal-barrier cell," Phys. Fl. 28, pp. 620-633, February 1985.

##### Reports

A. Wendt, "Saturation characteristics of counterstreaming warm electrons," ERL Memo No. UCBERL M85/45, 28 May 1985.

Talks at Eleventh International Conference on Numerical Simulation of Plasma, Montreal, Quebec, Canada, 25-27 June 1985:

C. K. Birdsall, W. S. Lawson, T. Crystal, S. Kuhn, N. Otani, I. Roth, and A. B. Langdon, "Problems of bounded particle simulations and first generation solutions," presented by Lawson, paper 3.A.01.

B. I. Cohen, M. E. Stewart, and C. K. Birdsall, "Direct implicit particle simulation of tandem mirror," paper 3.B.14.

Poster papers at Sherwood Theory Conference, April 15-17, University of Wisconsin, Madison, Wisconsin (abstracts follow). The paper by Theilhaber was also given at the International Conference on Stochasticity and Turbulence in Plasmas, March 26-29, 1985, Institute for Theoretical Physics, University of California, Santa Barbara.

##### Visits

C. K. Birdsall spent most of January and February visiting at (trip report available on request)

(1) Max Planck Institute for Plasma Physics, Garching, West Germany, working in the ASDEX group under Dr. Karl Lackner and especially with Dr. Roland Chodura, on plasma-wall interactions,

and

(2) Institute for Theoretical Physics, Innsbruck, Austria working with Dr. Siegbert Kuhn, also on plasma-wall interactions.

C. K. Birdsall taught a course on Numerical Plasma Simulation, 10-21 June, at the Spring College on Plasma Physics (Charged Particle Transport in Plasmas) at the International Centre for Theoretical Physics, Trieste, Italy. (20 hours of lecture, 7 projects, hands on)

Numerical Simulations of "Turbulent Trapping" and the Bump-on-Tail Instability. K. Theilhaber, Electronics Research Laboratory, University of California, Berkeley, CA 94720; D. Pesme and G. Laval, Centre de Physique Théorique, Ecole Polytechnique, 91128 Palaiseau, France.

Theoretical studies (1) strongly suggest that in the presence of sufficient turbulence, the growth rate of the weak warm-beam instability is significantly modified from its quasilinear value, and that a concurrent modification of velocity-space diffusion should occur. The criterion is approximately  $(k^2 D)^{1/3} > \gamma$ , where  $D$  is the quasilinear diffusion coefficient, and  $\gamma$  the quasilinear growth rate. This is in fact a regime always attained after a sufficient number of e-foldings. We numerically study the old paradigm of quasilinear theory by starting the instability in the presence of an initial turbulence, for a one-species, one-dimensional configuration. We shall present results for growth-rates, diffusion, and the correlation functions of the distribution function. In particular, we shall show the links to the "clump" turbulence of T.H. Dupree and co-workers (2).

- (1) G. Laval and D. Pesme, Phys. Rev. Letters, 53, 3, 270 (1984).
- (2) T.H. Dupree, Phys. of Fluids, 15, 334 (1972).

## Simulations of the Effect of ICRF Waves on the Interchange Instability\*

Niels F. Otani  
Electronics Research Laboratory  
University of California  
Berkeley, CA 94720

Recent results from the Phaedrus experiment at Wisconsin suggest that stabilization of the interchange mode in mirror plasma may be possible using RF waves excited externally in the vicinity of the ion-cyclotron frequency.<sup>1</sup> Two simulation codes have been developed for the purpose of studying the effect of ICRF waves on the linear growth rate of the interchange instability. Both codes model essentially the same system. The simulation plane is oriented perpendicular to the background magnetic field. An external gravitational field is fixed antiparallel to the density gradients initially present in the system. Full dynamics of the ions are followed while the electrons are represented as a cold  $\mathbf{E} \times \mathbf{B}$  fluid. The plasma is assumed quasineutral and the Darwin approximation is made. In the original code, no significant stabilization is observed for long interchange wavelengths ( $kL_n \leq 1$ ) and large RF fields ( $e^2 \nabla |E|^2 / 4m_i^2 \omega^2 g \approx O(1)$ ). The parameters required for tests of the effects on short wavelength modes ( $kL_n \gg 1$ ) excite numerical instabilities which appear related to an insufficiently accurate representation of the Lorentz force. A new code employing a different algorithm is being developed to bypass this problem. Supporting theory will also be presented.

\*Work supported by DOE Contract No. DE-AT03-76ET53064. Computations facilities provided by the National Magnetic Fusion Energy Computer Center.

<sup>1</sup>J. R. Ferron, N. Hershkowitz, R. A. Breun, S. . Golovato, and R. Goulding. Phys. Rev. Lett. 51, 1955 (1983).

A MODEL OF THE PLASMA-SHEATH REGION INCLUDING  
SECONDARY ELECTRON EMISSION AND ION REFLECTION\*

L.A.Schwager and C.K.Birdsall

Plasma Theory and Simulation Group  
Electronics Research Laboratory  
University of California, Berkeley CA 94720

A low temperature plasma interacts with a collector plate primarily through the emission of secondary electrons and the reflection of plasma ions. These phenomena affect the electrostatic potential drop across the sheath region and hence plasma transport to the plate. The computer code PDW1 models this behavior. The code is a one-dimensional, time-dependent electrostatic particle simulation. Particle ions and electrons, with a reduced mass ratio, are injected continuously from a plasma region into a plate where ions are reflected or cold electrons are emitted. A parametric study of the dependence of potential drop on interaction coefficient and mass ratio is presented. We have also developed theory for the effect on potential of ion reflection, for the cases of  $T_i=0$  and  $T_i=T_e$ , and of secondary electron emission for  $T_i=T_e$ . The simulation results for ion reflection approach those of our theory for the cold ion case. The simulation results with secondary electrons compare well with previous theory<sup>1</sup> for cold ions and demonstrate charge saturation as predicted.

<sup>1</sup>G.D.Hobbs and J.A.Wesson, Plasma Physics, Vol.9, 86 (1967)

\*Work supported by U.S.Department of Energy under contract DE-AT03-76ET53064.  
Computation facilities provided by NMFECC.

# DISTRIBUTION LIST

Argonne National Laboratory  
Brooks

Austin Research Associates  
Roberson

Bell Telephone Laboratories  
Hasegawa

Berkeley Research Assoc.  
Brecht, Orens, Thomas

Berkeley Scholars, Inc.  
Ambrosiano

Bhabha Research Centre  
Gioel

Cal. Inst. of Technology  
Bridges, Gould, Liewer

Cal. State Polytech. Univ.  
Rathmann

Cambridge Research Labs.  
Rubin

Centro de Electrodinamica, Lisbon  
Brinca

Columbia University  
Chua

Culham Laboratory  
Eastwood

Dartmouth  
Crystal, Hudson, Lotko

Department of Energy  
Hitchcock, Macrusky, Nelson,  
Sadowski

Ecole Polytechnique, Lausanne  
Hollenstein

Ecole Polytechnique, Palaiseau  
Adam

E.P.R.I.  
Scott

Ga Technologies  
Evans, Helton, Lee

Hascomb Air Force Base  
Rubin

Hewlett-Packard Laboratories  
Gleason, Moreoux

Hiroshima University  
Tanaka

Hughes Aircraft Co., Torrance  
Adler, Longo

Hughes Research Lab., Malibu  
Harvey, Hyman, Poeschel,  
Schumacker

I.N.P.E.  
Bittencourt, Montes

Institute of Fusion Studies  
Librarian

IPP-KFA  
Reiter

JAYCOR  
Hobbs, Tumolillo

Kirtland Air Force Base  
Pettus

Kyoto University  
Abe, Jimbo, Matsumoto

Lawrence Berkeley Laboratory  
Cooper, Kaufman, Kunkel, Lee

DISTRIBUTION LIST (cont.)

Lawrence Livermore National Laboratory

Albritton, Anderson, William Barr,  
Brengle, Bruijnes, Byers, Chambers,  
Chen, B. Cohen, R. Cohen, Denavit,  
Estabrook, Fawley, Fowler, Friedman,  
Fries, Fuss, Hewett, Killeen,  
Langdon, Liasinski, Matsuda, Max,  
Nevins, Nielsen, Smith, Tull

Massachusetts Institute of Technology

Berman, Bers, Gerver, Lane

Max Planck Inst. für Plasmaphysik

Biskamp, Chodura

Mission Research Corporation

Godfrey, Mostrom

Nagoya University

Kamimura, Research Info. Center

Naval Research Laboratory

Boris, Haber, Joyce, Winsor

New York University

Grad. Harned, Otani, Weitzner

Northeastern University

Chon, Silevitch

Oak Ridge National Lab.

Fusion Energy Library, Meier,  
Mook

Osaka University

Mima, Nishihara

Oxford University

Allen, Benjamin

Princeton Plasma Physics Lab.

Chen, Cheng, Lee, Okuda, Tang

Physics International

Woo

Riso National Laboratories

Lynov, Pecseli

SAI Corporation - Boulder

D'Ippolito, Myra

SAI Corporation - Palo Alto

Siambis

SAI Corporation - Virginia

Drobot, Mankofsky, McBride,  
Smith

Sandia Labs, Albuquerque

Freeman, Poukey, Quintenz, Wright

Shizuoka University

Saek

Stanford University

Blake, Buneman, Gledhill,  
Physics Library, Storey

Tel Aviv University

Cuperman

Tohoku University

N. Sato

TRW

Wagner

University of Arizona

Morse

Universität Bochum

Bochum

University of California, Berkeley

Arons, Birdsall, Chorin, Haller,  
Hess, Lawson, Lichtenberg,  
Lieberman, Morse, Theilhaber,  
Wendt

University of California, Davis

DeGroot

DISTRIBUTION LIST (cont.)

University of California, Irvine  
Rynn

Universität Innsbruck  
Cap, Kuhn

University of Iowa  
Knorr, Nicholson

Universität Kaiserslautern  
Wick

University of Maryland  
Gillory, Rowland

University of New Mexico  
Anderson, Humphries

University of Pittsburgh  
Zabusky

University of Southern California  
Kuehl

University of Texas  
Horton, Lebouef, McMahon,  
Tajima

University of Toronto  
Stangeby

University of Tromso  
Armstrong, Trulsen

Varian Associates  
Helmer

END

12-86

DTIC